2-26-2022

Precipitation and temperature extremes and association with large-scale climate indices: An observational evidence over India

S REHANA

PRANATHI YELESWARAPU

GHOUSE BASHA

Francisco Munoz-Arriola

© Indian Academy of Sciences

Precipitation and temperature extremes and association with large-scale climate indices: An observational evidence over India

S Rehana[1],*[ID], Pranathi Yeleswarapu[1], Ghouse Basha[2]
and Francisco Munoz-Arriola[3]

[1]*Hydroclimatic Research Group, Lab for Spatial Informatics, International Institute of Information Technology, Hyderabad, India.*
[2]*Department of Space, National Atmospheric Research Laboratory, Pakala, Tirupathi, India.*
[3]*Biological Systems Engineering, University of Nebraska-Lincoln, Lincoln, Nebraska, USA.*
Corresponding author. e-mail: rehana.s@iiit.ac.in

Climate change exposes more frequent natural hazards and physical vulnerabilities to the built and natural environments. Extreme precipitation and temperature events will have a significant impact on both the natural environment and human society. However, it is unclear whether precipitation and temperature extremes increase physical vulnerabilities across scales and their links with large-scale climate indices. This study investigates the relationship between precipitation and temperature extremes, as recommended by the Expert Team on Climate Change Detection and Indices (ETCCDI), and large scale climatological phenomenon indices (Indian Summer Monsoon Index (ISMI), Arctic Oscillation (AO), and North Atlantic Oscillation (NAO)), using India as a case study. Our findings show that extreme warm indices were primarily negatively related to ISMI and positively related to extreme cold indices. According to Pearson's correlation coefficients and Wavelet Transform Coherence (WTC), extreme warm indices were negatively related to ISMI and positively related to extreme cold indices. The extreme precipitation indices had a significant positive relationship, primarily with AO. Furthermore, from 1951 to 2018, India experienced an increase in warm extremes over western, central, and peninsular India, while cold indices increased over northwest India. Precipitation extremes of more than one day, more than five days, very wet and extremely wet days have increased across India except in the Indo-Gangetic plains, while heavy and very heavy precipitation days, consecutive wet days, and consecutive dry days have decreased.

Keywords. ETCCDI; precipitation; temperature; teleconnections; ISMI; AO.

1. Introduction

It has always been an important aspect where researchers strive to understand how and why climate extremes have changed in the past. The increase in precipitation extremes is evident in most parts of the globe due to an increase in atmospheric water holding capacity under warming climate based on both observations and climate model simulations (Utsumi *et al.* 2011; Vinnarasi and Dhanya 2016). Globally, understanding past changes in the characteristics of

extreme climate events, including recent changes in the intensity of heavy precipitation and temperature extremes, became critical for reliable projections of future changes (Donat *et al.* 2013; Panda *et al.* 2017; Lin *et al.* 2017; Vinnarasi *et al.* 2017).

In recent decades, India experienced several extreme events such as floods (Mishra *et al.* 2015) and heat waves (Murari *et al.* 2015; Rohini *et al.* 2016). Numerous studies adopted various indices to analyze and characterize Indian monsoon rainfall extremes in terms of intensity, frequency (Rajeevan *et al.* 2008) and spell (Dash and Mamgain 2011) based on fixed thresholds (Vinnarasi and Dhanya 2016) and statistics (Ghosh *et al.* 2012). A few studies used percentile thresholds (Panda *et al.* 2017) and fixed thresholds (Deshpande *et al.* 2016) at various spatial resolutions and scales to estimate temperature extremes. Most of these studies support that climate extremes for India have changed drastically with various methods and huge number of indices. However, how best to define the standard climate extreme is debatable (Alexander 2016). Studies related to climate extremes have progressed enormously over the last few decades all over the world (Donat *et al.* 2013; Curry *et al.* 2014) due to coordinated international efforts led by the Expert Team on Climate Change Detection and Indices (ETCCDI) (table 1). Over Indian region, few studies attempted to analyze the trends of rainfall and temperature extremes at river basin scales (Chandrashekar and Shetty 2018; Das and Nanduri 2018; Dimri 2019; Khan *et al.* 2019), and all over India with modified forms of ETCCDI indices (Panda *et al.* 2016), current and future scenarios of threshold-based precipitation (R90, R95, R99, R1, R5, R10, etc.) and temperature (TX90, TX95, TX99, etc.) (Kumar *et al.* 2020). For example, Kumar *et al.* (2020) used various modified forms of ETCCDI indices of precipitation such as R90, R95, R99, R1, R5, R10, and temperature indices such as TX90, TX95, TX99. Roy (2019) used four seasonal extreme temperature indices (DTR, WSDI, TX90p, SU, TX10p, TN90p, TR) for a period of 1980–2010 using station-based observations. Rai *et al.* (2019) studied spatio-temporal variability of projected precipitation extremes using four ETCCDI (CDD, CWD, R20mm, R95p) indices using Coordinated Regional Climate Downscaling Experiment-South Asia domain (CORDEX-SA) data. Most of these studies reported the spatio-temporal trends of precipitation and temperature extremes independently. However, none of the studies have explored the spatio-temporal trends of both precipitation and temperature indices in terms of

intensity, frequency, and durations based on the most dependable station-based observations in their original formulations altogether. Therefore, the current study aims to investigate the variability of 10 precipitation and 13 extreme temperature indices developed by ETCCDI over India using gridded temperature and precipitation data sets from the India Meteorological Department (IMD). These indices are classified as intensity indices, absolute threshold indices, relative threshold indices, duration indices, and so on (Yang *et al.* 2018).

Further, we have also investigated the relation between extreme precipitation and temperature indices with large scale oscillations (e.g., Southern Oscillation Index (SOI), Pacific Decadal Oscillation (PDO), Dipole Mode Index (DMI), Arctic Oscillation (AO), North Atlantic Oscillation (NAO) and Indian Summer Monsoon Index (ISMI)). Therefore, the specific objectives of the study were to (1) analyze the spatio-temporal variability of annual precipitation and temperature extremes over India with the most dependent station based on observed historical data; (2) estimate the possible trends of precipitation and temperature extremes from 1951 to 2018; (3) explore the relationships of precipitation and temperature extremes with large scale climatological phenomenal indices, employing wavelet transform coherence.

2. Methodology

To analyze the spatio-temporal variabilities of precipitation and temperature extremes, the annual time-series of each index for a period of 1951–2018 was estimated for each grid point and analyzed for all over India. To study the spatio-temporal trends of each precipitation and temperature extremes, we performed Mann–Kendall trend test to assess the significance of monotonic trends; Sen's slope to estimate the magnitude and to characterize the trend as increasing or decreasing of a continuous annual time series data for a period of 1951–2018. To study the relationships of precipitation and temperature extremes with large-scale climatological phenomenal indices, we adapted Pearson's correlation coefficients and Wavelet Transform Coherence measures. The study considered 10 precipitation and 13 extreme temperature indices (table 1) in the analysis of spatio-temporal variability, possible trends and association with climate indices.

Table 1. *List of expert team for climate change detection monitoring and indices (ETCCDMI) of precipitation and temperature indices.*

ID (unit)	Indicator name	Definitions	Mean (range)
SU25 (days)	Summer days	Annual count when TX (daily maximum) > 25°C	323.84 (311.26–336.34)
TR20 (days)	Tropical nights	Annual count when TN (daily minimum) > 20°C	196.4 (179.4–219.16)
TXx (°C)	Hottest days	Monthly maximum value of daily maximum temp	34.14 (33.27–35.32)
TNx (°C)	Warmest nights	Monthly maximum value of daily minimum temp	21.76 (20.95–22.82)
TXn (°C)	Coldest days	Monthly minimum value of daily maximum temp	27.3 (26.48–28.50)
TNn (°C)	Coldest nights	Monthly minimum value of daily minimum temp	16.12 (15.34–17.1)
TN10p (% days)	Cool nights	Percentage of days when TN < 10th percentile	24.98 (10.12–42.6)
TX10p (% days)	Cool days	Percentage of days when TX < 10th percentile	26.79 (13.23–44.72)
TN90p (% days)	Warm nights	Percentage of days when TN > 90th percentile	34.89 (17.74–55.64)
TX90p (% days)	Warm days	Percentage of days when TX > 90th percentile	35.24 (17.69–55.48)
WSDI (days)	Warm spell duration indicator	Annual count of days with at least 6 consecutive days when TX > 90th percentile	77.93 (29.0–145.6)
CSDI (days)	Cold spell duration indicator	Annual count of days with at least 6 consecutive days when TN < 10th percentile	39.32 (4.5–86.93)
DTR (°C)	Diurnal temperature range	Monthly mean difference between TX and TN	12.1 (11.4–12.7)
RX1day (mm)	Max 1-day precipitation amount	Monthly maximum 1-day precipitation	24.5 (21.18–28.3)
Rx5day (mm)	Max 5-day precipitation amount	Monthly maximum consecutive 5-day precipitation	48.3 (41.22–56.7)
SDII (mm/day)	Simple daily intensity index	Annual total precipitation divided by the number of wet days (defined as PRCP >= 1.0 mm) in the year	13.25 (12.04–14.32)
R10mm (days)	Number of heavy precipitation days	Annual count of days when PRCP >= 10 mm	32.58 (26.38–39.21)
R20mm (days)	Number of very heavy precipitation days	Annual count of days when PRCP >= 20 mm	16.89 (13.6–20.76)
CDD (days)	Consecutive dry days	Maximum number of consecutive days with RR < 1 mm	77.83 (53.22–98.19)
CWD (days)	Consecutive wet days	Maximum number of consecutive days with RR >= 1 mm	13.76 (10.6–16.7)
R95p (mm)	Very wet days	Annual total PRCP when RR > 95th percentile	402.8 (269.4–561.38)
R99p (mm)	Extremely wet days	Annual total PRCP when RR > 99th percentile	333.68 (233.9–467.6)
PRCPTOT (mm)	Annual total wet-day precipitation	Annual total PRCP in wet days (RR >= 1 mm)	1125.00 (909.98–1344.9)

2.1 *Spatio-temporal variabilities of precipitation and temperature extremes*

The annual precipitation and temperature extreme time-series estimated for each cell for a period of 1951–2018 was used to study the spatial distribution of extremes all over India. Furthermore, such annual time series of precipitation and temperature extremes were used to estimate the spatial averages covering all valid cells within India to study the temporal variability of each extreme index for a long observational data from 1951 to 2018. Using both precipitation and temperature extremes of each index at annual scales, the study reported spatio-temporal variability for all over India with the most dependable and long time period observed station-based data.

2.2 *Spatio-temporal trends analysis of precipitation and temperature extremes*

The significance levels of trends are checked at 5% significance level and the percentage of grids showing significant trends for precipitation and temperature indices all over India are discussed. Non-parametric Mann–Kendall trend test was applied to detect monotonic trends in precipitation and temperature extremes, and the spatially averaged slope of linear trends is estimated using Sen's slope method. The Mann–Kendall trend analysis is a non-parametric test (Mann 1945; Kendall 1955) to assess if there is an upward (positive) or downward (negative) trend of a variable of interest over time for a given significance level. The test compares the relative magnitudes of sample data rather than the data values themselves (Gilbert 1987). The following procedure explains the Mann–Kendall trend test:

- The time series, x_i, of the variable for which the trend test to be applied is considered as an ordered time series.
- Each of the data point, x_i, is compared with all the subsequent data values to estimate the Mann–Kendall statistic, S, as follows:

$$S_i = \sum_{i=2}^{n} \sum_{j=1}^{i-1} \text{sign}(x_i - x_j), \qquad (1)$$

where

$$\text{sign}(x_i - x_j) = \begin{cases} 1 & \text{if} \quad x_i > x_j \\ 0 & \text{if} \quad x_i = x_j \\ -1 & \text{if} \quad x_i < x_j \end{cases} \qquad (2)$$

- A very high positive value of S indicates an increasing trend, and a very low negative value indicates a decreasing trend.
- From the Mann–Kendall statistic, S, the normalized test statistics, Z, is computed as follows:

$$Z = \frac{S - 1}{[VAR(S)]^{1/2}} \quad \text{if } S > 0, \qquad (3)$$

$$Z = 0, \qquad\qquad \text{if } S = 0, \qquad (4)$$

$$Z = \frac{S + 1}{[VAR(S)]^{1/2}}, \quad \text{if } S < 0, \qquad (5)$$

where $VAR(S)$ is the variance of S. According to Kendall (1955), $VAR(S)$ can be written as follows:

$$VAR(S) = \frac{1}{18}\Bigg[n(n - 1)(2n + 5) \\ - \sum_{p=1}^{g} t_p(t_p - 1)(2t_p + 5)\Bigg], \qquad (6)$$

where n is the number of data points, g is the number of tied groups (a tied group is a set of sample data having the same value), and t_p is the number of data points in the Pth group. The Z-value follows a standard normal distribution. For testing the decreasing or increasing trend, a significance level α is used. The probability associated with the computed test statistics, Z-value, is estimated. The trend is identified as decreasing if Z-value is negative and the computed probability is less than the level of significance, and the trend is identified as increasing if the Z-value is positive and the computed probability is less than the level of significance. If the computed probability is greater than the level of significance, then there is no trend.

Once the possible trends have been identified, it is important to estimate the magnitude of trend or change per unit time, Q_{sen}, which can be established using a non-parametric method proposed by Sen (1968) and Hirsch *et al.* (1982). The magnitude of the slope or change per unit time, Q_{sen} can be estimated by considering the slopes of all data pairs are as follows:

$$Q_{\text{sen}} = \text{Median}\left[\frac{Y_i - Y_j}{X_i - X_j}\right], \, i = 1, 2, \ldots, N, \;\; \forall j < i, \qquad (7)$$

where Y_i and Y_j are data points at X_i and X_j, respectively. If there are n values of X_i in the time

series, then there will be $(n(n-1)/2)$ slopes estimates. The Sen's estimator of slope is the median of these n values of Q_{sen}. The positive and negative signs of Q_{sen} represent increasing and decreasing trends, respectively.

2.3 *Dependence of precipitation and temperature extremes with climatological phenomenal indices: Wavelet transform coherence (WTC)*

The WTC has emerged as new signal analysis which can combine wavelet transform with cross-spectrum analysis to measure the covarying relationships of hydroclimatological variables in recent years (Irannezhad *et al.* 2020; Jena *et al.* 2020). The wavelet transform coherence (WTC) is employed to explore the dependency of the large-scale climate indices and precipitation and temperature indices over India in the time–frequency domain. The WTC can combine the wavelet transform and cross-spectrum analysis to measure the significant dependency between the climate and precipitation and temperature extremes. The WTC between two-time series can represent the localized correlation coefficient in time–frequency space; following Torrence and Compo (1998), WTC can be defined as follows:

$$R_n^2(s) = \frac{\left|S\left(s^{-1} W_n^{XY}(s)\right)\right|^2}{S\left(s^{-1}\left|W_n^X(s)\right|^2\right) \times S\left(s^{-1}\left|W_n^Y(s)\right|^2\right)}, \tag{8}$$

where x_n and y_n are two-time series, with cross wavelet transform as $W^{XY} = W^X W^{Y*}$, where $*$ denotes complex conjugation. S denotes a smoothing operator as follows:

$$S(W) = S_{scale}(S_{time}(W_n(s))). \tag{9}$$

S_{scale} is smoothing along the wavelet scale axis and S_{time} as smoothing over time. A suitable wavelet for this purpose can be Morlet wavelet with smoothing operator, following Torrence and Compo (1998) as follows:

$$\begin{aligned} S_{time}(W)|_s &= \left(W_n(s) \times c_1^{\frac{-t^2}{2s^2}}\right)\Big|_s, \\ S_{time}(W)|_s &= \left(W_n(s) \times c_2 \prod(0.6s)\right)\Big|_n. \end{aligned} \tag{10}$$

c_1 and c_2 are normalized constants and the factor 0.6 is empirically determined scale decorrelation length for the Morlet wavelet. To measure the statistical dependency between various climate indices and precipitation and temperature extreme indices, this study used Pearson's correlation coefficient (r). The statistically significant $(p < 0.05)$ Pearson's correlation coefficients were estimated and considered as a reference to study the dependence analysis using WTC. The initial dependency analysis between various precipitation, temperature extremes and large-scale climatological indices (teleconnections) was carried out based on Pearson's correlation coefficients. However, to know the localized correlation coefficients and their evolution over a continuous time–frequency space, and to identify the interaction between the selected combinations of extremes based on the Pearson's correlation coefficients, we performed WTC analysis.

3. Data

3.1 *Data sources and quality controls*

The present study tried to use a high resolution $(0.25° \times 0.25°)$ daily rainfall data prepared by India Meteorological Department (IMD) for the period of 1951–2018 for a spatial domain of 6.5°–38.5°N and 66.5°–100°E, covering mainland region of India. The daily rainfall records are generated from 6955 rain gauge stations with varying availability and the density of the stations is relatively high in the southern peninsula and relatively low over northernmost areas of the country, i.e., northwest India, northeast India, and eastern parts of central India (Pai *et al.* 2014). The daily maximum and minimum temperature data set at $1°\times1°$ resolution for the period of 1951–2018 from India Meteorological Department (IMD) are used in the present study. The maximum and minimum temperature data sets are brought to a common resolution of $0.25°\times0.25°$ at precipitation gridded data set by using bilinear interpolation without compromising the spatial variability of the data sets. A total of 4964 grids all over India are considered to study the precipitation and temperature extreme indices.

To identify the relation between temperature/precipitation indices with large scale teleconnections, we have chosen the Southern Oscillation Index (SOI), Pacific Decadal Oscillation (PDO), Dipole Mode Index (DMI), Arctic Oscillation (AO), North Atlantic Oscillation (NAO), Indian

Summer Monsoon Index (ISMI) for a period of 1951–2018. The Southern Oscillation Index (SOI) can be obtained from http://www.bom.gov.au/climate/current/soihtm1.shtml, which represents the observed surface air pressure difference between western (Tahiti) and eastern tropical Pacific (Darwin, Australia) during El Niño and La Niña episodes. The Pacific Decadal Oscillation (PDO) can be downloaded from https://www.ncdc.noaa.gov/teleconnections/pdo/data, which represents long-lived El Niño like pattern of Pacific climate variability. The Dipole Mode Index (DMI) data can be downloaded from http://www.jamstec.go.jp/frcgc/research/d1/iod/DATA/dmi.monthly.txt. The DMI is the difference in sea surface temperature (SST) between the western and eastern equatorial Indian Ocean. The Arctic Oscillation (AO) represents the Northern hemisphere annular mode and can be obtained from https://www.ncdc.noaa.gov/teleconnections/ao/data.json. The North Atlantic Oscillation (NAO) index is a major model of variability, referring to the sea pressure difference between sub-tropical high surface pressure and sub-polar low surface pressures, centered on Iceland, obtained from https://crudata.uea.ac.uk/cru/data/nao/. The Indian Summer Monsoon Index (ISMI) is defined as the averaged total rainfall during the monsoon period of June–September (JJAS) over the Indian subcontinent, which can be obtained from http://apdrc.soest.hawaii.edu/projects/monsoon/seasonal-monidx.html. All these indices are extracted at monthly time scale for a period of 1951–2018.

4. Extreme precipitation and temperature indices

The precipitation and temperature extreme indices adopted in the analysis have been based on the Expert Team on Climate Change Detection and Indices (ETCCDI), which is a joint group of the World Metrological Organization (WMO) Commission for Climatology (CCI), the World Climate Research Programme (WCRP) and the Joint Commission for Ocean Monitoring (JCOMM) (https://www.wcrp-climate.org/etccdi), with a suite of 23 indices derived from daily precipitation, maximum and minimum temperatures as represented in table 1. These indices are widely used in several assessment studies, representing the more extreme ends of the probability distributions and the changes in intensity, frequency and duration

(Zhang *et al.* 2011). Totally 10 precipitation and 13 temperature indices are proposed by ETCCDI. The CCI-CLIVAR Expert Team for Climate Change Detection and Indices (ETCCDI) made efforts to estimate extreme climate indices based on daily temperature and precipitation data. There are about 16 temperature extreme indices which can be broadly classified as threshold-based indices (FD0, SU25, ID0, TR20, GSL, TN10p, TX10p, TN90p, TX90p), intensity-based indices (TXx, TNx, TXn, TNn, DTR), and duration-based indices (WSDI, CSDI) (refer to table 1). All these extreme temperature indices have its significance related to crop yield, heat waves and water resources management. Warm Spell Duration Index (WSDI), which is defined as annual count of days with at least six consecutive days when TX > 90th percentile (table 1), was considered as a proxy for the duration of heat waves over India (Yaduvanshi *et al.* 2021). The temperature indices such as GSL (growing season length), FD (number of frost days), and ID (number of icing days) have shown non-significant trends, and these indices are not suitable indices for Indian weather (Vinnarasi *et al.* 2017). The present study considered about 13 threshold-based (SU25, TR20, TN10p, TX10p, TN90p, TX90p), intensity-based (TXx, TNx, TXn, TNn, DTR), and duration-based (WSDI, CSDI) extreme indices to study the spatio-temporal variability of temperature extremes all over India (table 1). The 13 temperature extremes were estimated for all over India for the period 1951–2018 and analysed for the spatio-temporal annual average variability.

Major precipitation indices which are used to measure the frequency of extreme precipitation events, not the actual amount of precipitation events, are consecutive dry days (CDD), consecutive wet days (CWD), number of very heavy precipitation days (R20mm), and very wet days (R95p) (Rai *et al.* 2019). Significant changes in extreme precipitation events such as monthly maximum 1-day and 5-day precipitation events such as RX1day and RX5day, respectively, very wet days (annual total precipitation, when rainfall >95th percentile) R95p, extremely wet days (annual total precipitation when rainfall > 99th percentile) R99p and annual total wet-day precipitation (annual total precipitation in wet days, rainfall > 1 mm). PRCPTOT would have an impact on agricultural production, flash flooding and ecosystems (Yaduvanshi *et al.* 2021). The present study considered 10 intensity-based

precipitation extreme indices (annual total wet day precipitation (PRCPTOT), max-1day precipitation amount (RX1day), and max-5day precipitation amount (RX5day)), threshold-based precipitation extreme indices (extremely wet days (R99p) and very wet days (R95p)), duration based precipitation extreme indices (consecutive wet days (CWD) and consecutive dry days (CDD)), and frequency-based precipitation extreme indices (Simple Daily Intensity Index (SDII), heavy (R10mm) and very heavy (R20mm) precipitation days) to study the spatio-temporal variability of precipitation extremes all over India (table 1). The 10 precipitation extremes were estimated for all over India for the period of 1951–2018 and analysed for the spatio-temporal annual average variability.

5. Results and discussion

5.1 *Spatial variation of precipitation and temperature extremes over India*

The annual spatial average of precipitation and temperature extreme indices estimated over a period of 1951–2018 is shown in figures 1 and 2, respectively. As discussed in the previous section, we have utilized the 10 precipitation extreme indices. Both the max-1day and max-5day precipitation amounts show similar spatial variability with higher magnitudes over the Western Ghats, north, central and East Coast, northeast parts of India, whereas lower magnitudes are observed over few parts of peninsular India and northwestern parts. The max-1day (max-5day) precipitation amounts have been found to be in the range of 21.18–28.3 mm (41.22–56.7 mm) with a spatial average value estimated as 24.5 mm (48.3 mm) for the period of 1951–2018 (table 1). The threshold-based precipitation indices such as very wet days (R95p) and extremely wet days (R99p) depict higher magnitudes over most of the country, except over northwestern. The annual total wet-day precipitation (PRCPTOT) amounts are found to be in the range of ~ 909.98–1344.9 mm with extremely high magnitudes over northeastern zone, central India and Western Ghats. Frequency-based precipitation indices (SDII, R10mm and R20mm) have higher magnitudes over Western Ghats and northeastern region of the country, with moderate magnitudes for the rest of the country (figure 1). The annual spatial variability of SDII was noted in the range of ~ 12.04 to ~ 14.32 mm with higher

magnitudes towards northwestern and Western Ghats, few parts of central and northeast India along with moderate values over the peninsular India. The spatial average of SDII estimated for all over India is ~ 13.25 mm. The spatial distribution of the number of heavy precipitation days (R10mm) is about ~ 39 days over Western Ghats and East Coast and northeast with lower magnitudes of about ~ 26 days over western parts of the country. Whereas, another frequency-based precipitation extreme index of R20mm, number of very heavy precipitation days, has higher magnitudes over Western Ghats and northeast parts of the country with an average ~ 17 days in terms of spatial distribution (table 1). Similar values are also reported over Western Ghats by Rai *et al.* (2019). The duration-based precipitation extreme index of consecutive dry days (CDD) has higher magnitudes over western, central and southern India of about ~ 98 days. The overall range of CDD was noted in the range of ~ 53–98 days with an average spatial distribution over India as ~ 79 days. Whereas, another duration-based precipitation index of consecutive wet days (CWD) has followed the pattern of frequency-based precipitation indices of heavy and very heavy precipitation indices with higher magnitudes over Western Ghats and northeastern zone. Overall, all wet precipitation extreme indices have been found to be more intense over Western Ghats and northeastern parts of India while intense dry indices prevail over the country's northern and western regions.

The spatial annual average values of temperature extreme indices were estimated over 68 years (1951–2018) from IMD gridded data, as illustrated in figure 2. Higher magnitudes of summer days (SU25) were estimated as about 336 days over southern part of India and with moderate magnitude all over the country, with spatial average of about ~ 324 days (figure 2a, table 1). The highest magnitudes of tropical nights (TR20) are found over the peninsular and central India and moderate magnitudes over the rest of the country with a spatial average of about ~ 196 days all over India. The highest magnitude of hottest days (TXx) was observed over the country's central and western regions (35.32°C). Higher magnitudes of the warmest nights (TNx) are found over the east and west coasts of the country, with a magnitude of 22.82°C (figure 2b and c). The coldest days (TXn) are found to be more pounced over major parts of the country, with minimum magnitudes over
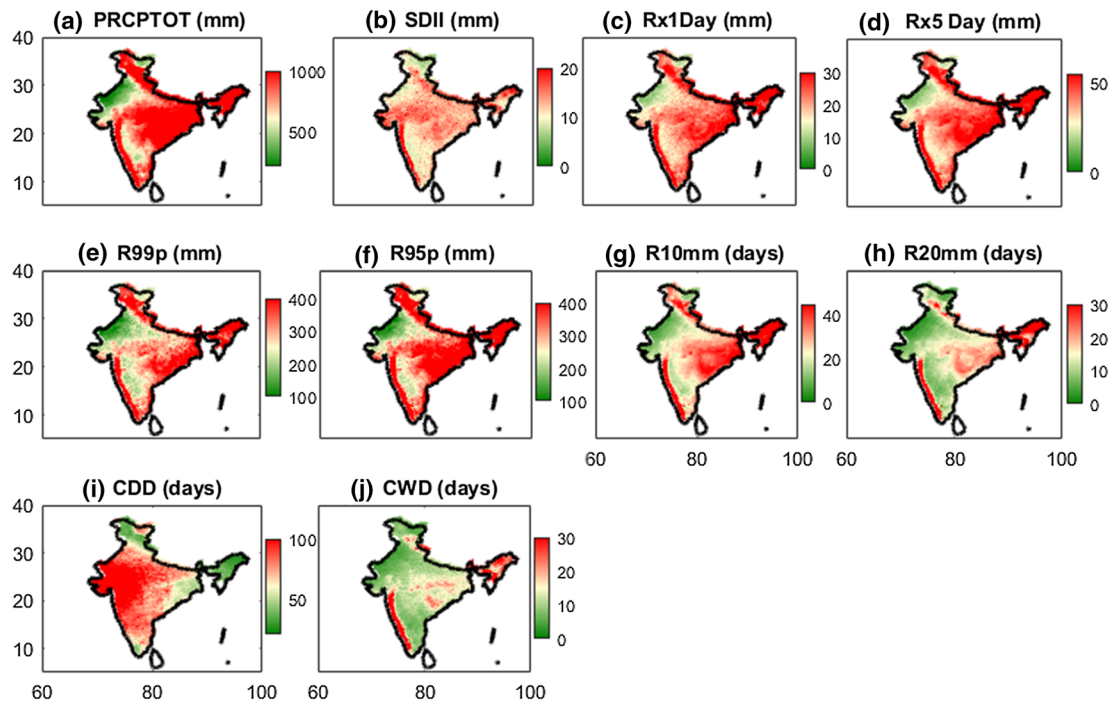
Figure 1. Annual average precipitation indices over India estimated for a period of 1951–2018. Precipitation indices: annual total wet day precipitation days (PRCPTOT), Simple Daily Intensity Index (SDII), max-1-day precipitation amount (RX1day), max-5-day precipitation amount (RX5day), extremely wet days (R99p), very wet days (R95p), heavy precipitation days (R10mm), very heavy precipitation days (R20mm), consecutive dry days (CDD), and consecutive wet days (CWD).
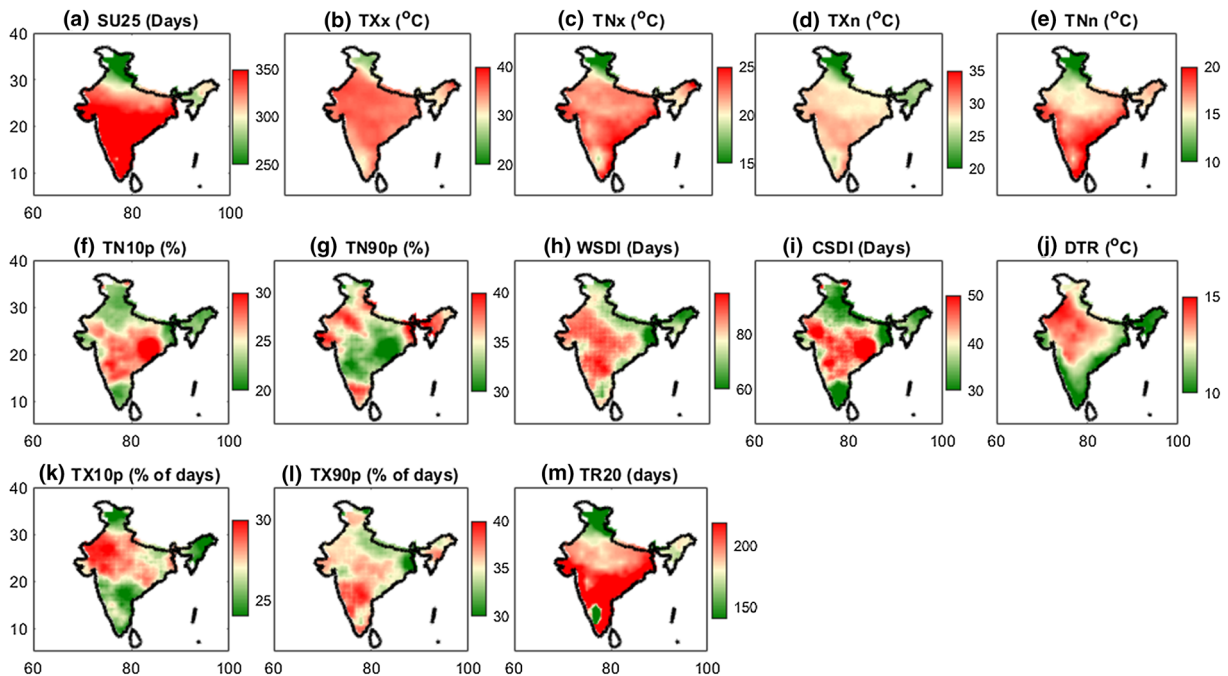

Figure 2. Annual average of extreme temperature indices over India estimated for 1951–2018. The extreme indices considered are summer days (SU25), hottest days (TXx), warmest nights (TNx), coldest days (TXn), coldest nights (TNn), percentage of cool nights (TN10p), percentage of warm nights (TN90p), warm spell duration indicator (WSDI), cold spell duration indicator (CSDI), daily temperature range (DTR), percentage of cool days (TX10p), percentage of warm days (TX90p), and tropical nights (TR20).

northeastern and Himalayan regions in the range of ~ 26.48–28.50°C. The spatial variability of coldest nights (TNn) is observed over southern parts (with

higher magnitude) and over northern India (with lower magnitudes) in the range of ~ 15.34–17.1°C (figure 2e, table 1). The percentage of cool nights

(TN10p) and warm nights (TN90p) shows similar spatial variability with highest magnitudes over southern and lower magnitudes over northern parts of India (figure 2f and g). The range of TN10p and TN90p were estimated as ∼10.12 to ∼42.6°C and ∼17.74 to ∼55.64°C throughout India. The duration-based temperature indices of warm spell duration index (WSDI) were found to be in the range of 29–146 days with spatial variability of higher magnitudes over few parts of peninsular, central, and northwestern parts of India, with lower magnitudes over northeastern and Himalayan states (figure 2h). The cold spell duration index (CSDI) was found to be between ∼4.5 and ∼87 days. The spatial distribution of higher magnitudes over central and northwestern parts of the country with lower magnitudes over few parts of southern states of Tamil Nadu, Kerala, and over northeastern states with spatial average value of 39.33 days (figure 2i). The daily temperature range (DTR) was found in the range of ∼11.4 to ∼12.7°C, having higher magnitudes over central and northwestern states of the country, with spatial average values estimated as ∼12.1°C as shown in figure 2(j) (table 1). Overall, the warm and cold temperature indices are prevailing moderately over most of the country, with higher magnitudes over northwestern and central parts of India, except over Himalayan states.

5.2 *Spatio-temporal trends of precipitation and temperature extremes over India*

The spatial distribution and spatially averaged temporal trends of extreme precipitation indices over India are shown in figures 3 and 4, respectively. The simple daily intensity index (SDII) (annual total precipitation/number of wet days) shows a significant increase over East Coast and western part of India. While there are significant negative trends in the northern zone, particularly in Uttar Pradesh, Uttarakhand, Delhi, and Himachal Pradesh (figure 3b). The spatial distribution of RX1day and RX5day extremes showed positive trends across most of the country, with the exception of northeastern and hilly Himalayan regions (figure 3c and d). The spatial trend shows that all over India CDD index has shown positive magnitude of slopes all over India with higher magnitudes over central India (figure 3i). The very heavy precipitation days (R20mm), heavy precipitation days (R10mm) and consecutive dry days

(CDD) do not show significant changes. The annual total wet day precipitation (PRCPTOT) and very wet precipitation amounts have shown more pronounced decreasing magnitude of trends over north India (figure 3a).

The spatial averaged annual extreme precipitation indices such as max-1day, max-5day, simple daily intensity index, very wet days, and extremely wet days have exhibited increasing trends, whereas the annual precipitation indices of number of heavy and very heavy precipitation days, consecutive wet days, and consecutive dry days have shown decreasing trends at a significance level of 0.05 (figure 4). Simple daily intensity index (SDII) shows an increasing trend over India by 0.08 mm/decade (figure 4b). After 1980, the wet extreme precipitation indices, very wet (R95p) and extremely wet (R99p), increased by 11.3 mm/decade and 7.1 mm/decade, respectively (figure 4e, f). As per the study of Kumar *et al.* (2020), about 13% of India has significant trends of R95p for a period of 1971–2017.

The CDD has shown decreasing trends at a rate of 0.3 days/decade in terms of spatial averaged scales all over the country (figure 4i). The wet index and annual consecutive wet days (daily precipitation >1 mm) (CWD) have exhibited a significant decreasing trend at 0.5 days/decade (figure 4j). Most of the precipitation extremes, simple daily intensity index, number of heavy and very heavy precipitation days, and very wet days, have shown similar spatial distribution with positive trends all over India and significant negative trends across north India. The positive changes in precipitation extremes (heavy rainfall indices of R20mm, R95p, RX5 and RX1 days) obtained in the present study were consistent with Yaduvanshi *et al.* (2021).

The spatial trend analysis for extreme temperature indices is shown in figure 5. The significant areas at 0.05 significant level with Sen's slope magnitude test were shown. The spatial averaged annual extreme precipitation indices such as summer days, hottest days, warmest nights, coldest days, coldest nights, warm nights, warm spell duration index, diurnal temperature range and warm days have exhibited increasing trends, whereas the cold indices such as cool nights, cold spell duration index, and cool days have shown decreasing trends. The number of summer days increased significantly over India's northern western zone and coastal parts, as well as the central-west zone, more specifically over Rajasthan,
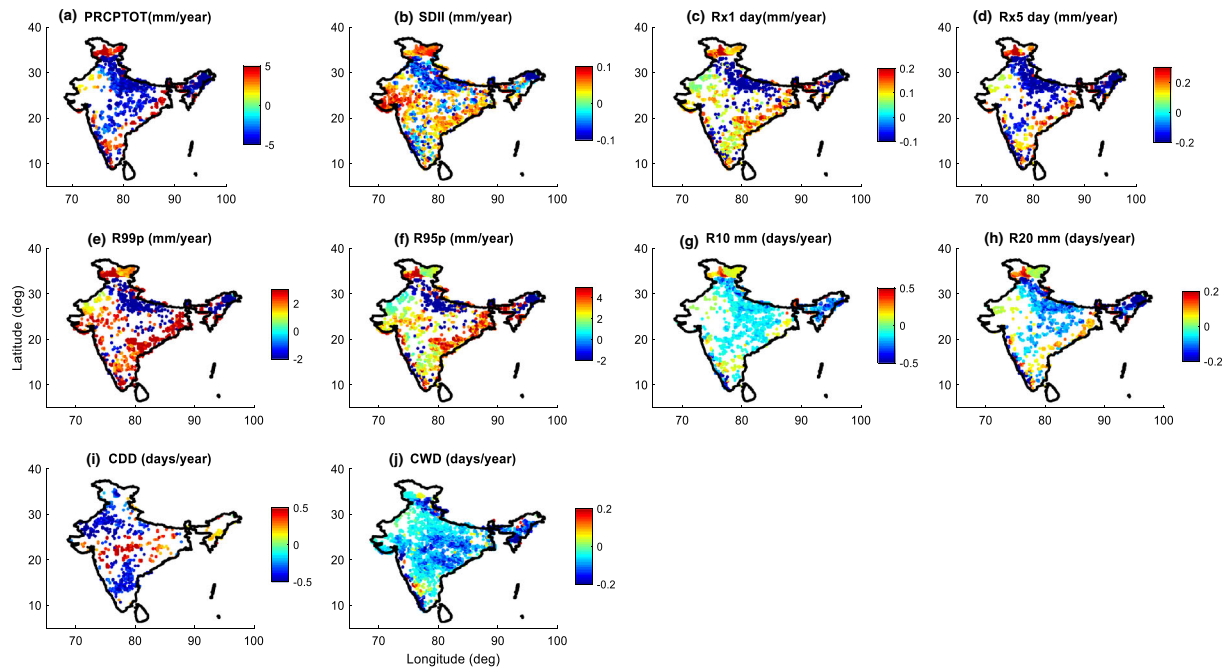
Figure 3. Spatial pattern of Sen's slope (magnitude) of annual trends of extreme precipitation indices over India at 5% significance level. Precipitation indices: max-1-day precipitation amount (RX1day), max-5-day precipitation amount (RX5day), extremely wet days (R99p), very wet days (R95p), very heavy precipitation days (R20mm), heavy precipitation days (R10mm), annual total wet day precipitation days (PRCPTOT), consecutive wet days (CWD), consecutive dry days (CDD), simple daily intensity index (SDII).

Gujarat, and Maharashtra (figure 5a). The hottest day (TXx) represents an increasing trend in most of the regions in India ($\sim 75\%$ of region). Similarly, the warmest nights (TNx) show a 0.05°C/decade increase trend. Compared to other regions of India, increasing trend in warmest nights is large over northwestern states. Both the intensity-based temperature extremes, hottest days and warmest nights have shown an increasing trend after 1990s. Similarly, the number of tropical nights showed increasing trends all over India with higher magnitudes over Rajasthan and Gujarat, except for northeastern and Himalayan regions. The percentile index, such as percentage of warm nights (TX90p), shows an increasing trend over India (about $\sim 80\%$ of the region) except for northeastern and eastern India. Southern India has experienced an increase in warm days for a period of 1951–2018. The warm nights (TN90p) percentile depicts an increasing trend (44% of the Indian region) at a rate of 1.5°C/decade (figure 2). High magnitude of increasing trends of warm nights was noted over Tamil Nadu, Kerala and northwestern states of Gujarat and Rajasthan. The warm index, WSDI exhibits an increasing trend of 75% of Indian region. The warm index, WSDI also shows a

positive increasing trend of 9.5 days/decade. The increasing trend is specifically confined to the western and southern regions of India. It is also noted that the maximum value of WSDI of about 145.6 days occurred in the year 2009, which is considered as one of the severe drought years all over India with about 37% of area was affected with drought based on Standardized Precipitation Evapotranspiration Index (SPEI) (Rehana and Monish 2020, 2021). The WSDI by definition represents the heat wave index and all over India increase of intensity and duration of heatwave indices are evident based on the earlier studies (e.g., Sharma and Mujumdar 2017). According to Ratnam *et al.* (2016), heat waves are common in southeastern coastal India and northcentral India. Heat wave changes have been significantly correlated with warming of Indian Ocean and teleconnections of ENSO (Rohini *et al.* 2016). The positive trend grids of DTR were distributed over coastal parts of central-west zones, and few parts of peninsular India, which is in convince with earlier research findings based on Vinnarasi *et al.* (2017).

The long-term variation along with trend analysis of extreme temperature indices is shown in figure 6. Both the hottest days and warmest nights
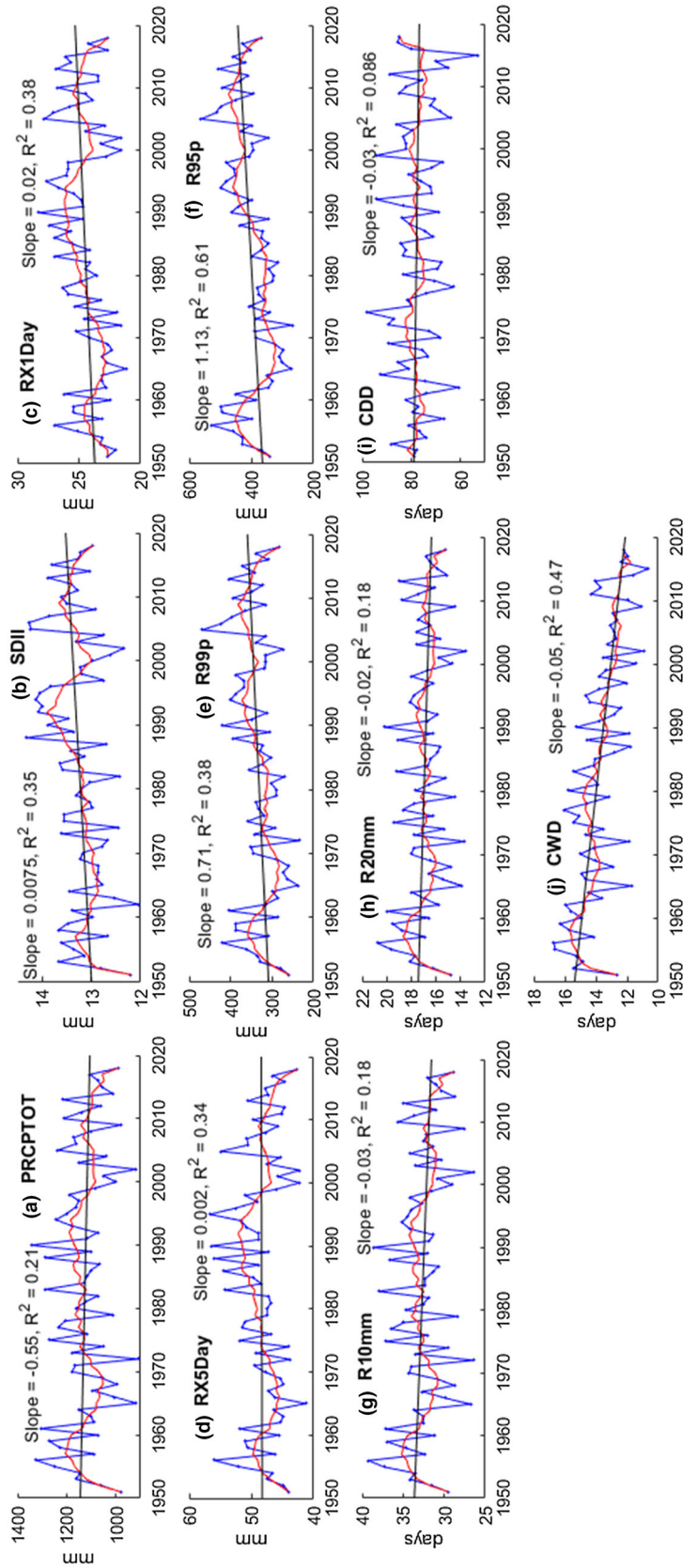
Figure 4. Annual spatial averaged precipitation extremes all over India for 1951–2018. The black solid line shows the linear trend line, red colour solid line is 10-yr moving average.
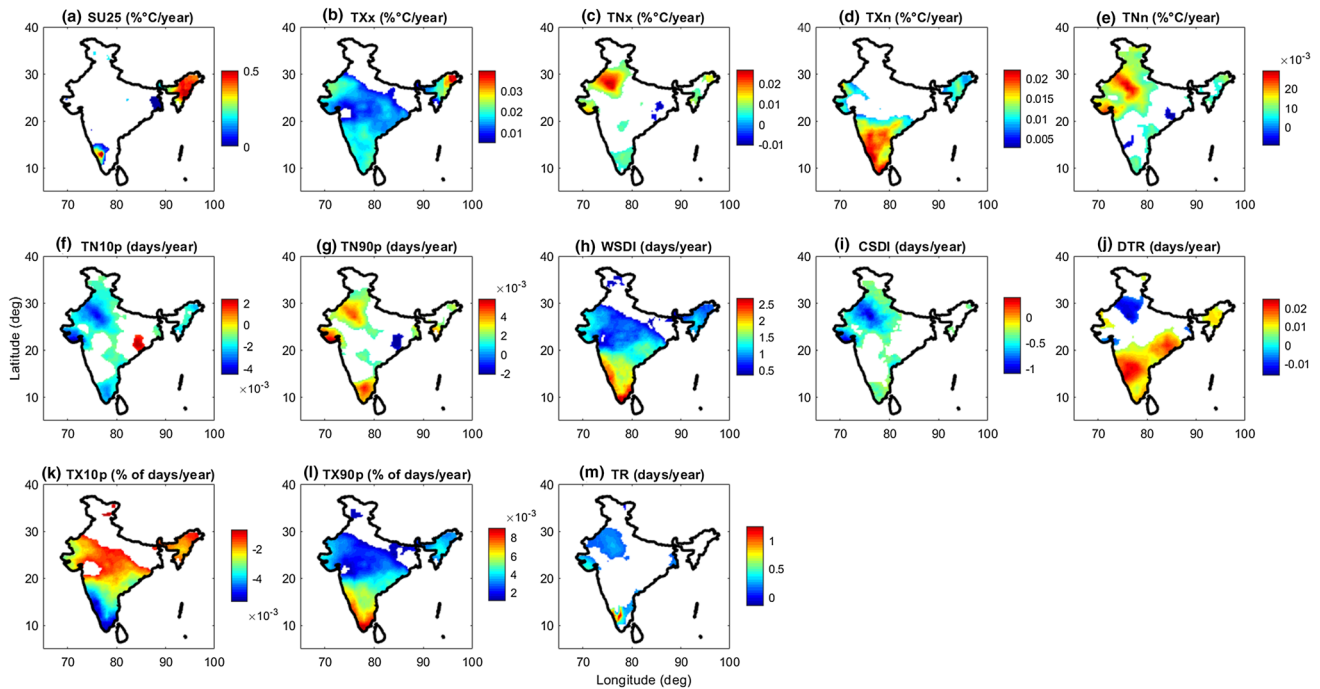
Figure 5. Spatial pattern of Sen's slope (magnitude) of annual trends of extreme temperature indices over India at 5% significance level. The extreme indices considered are warm spell duration indicator (WSDI), percentage of warm days (TX90p), percentage of cool days (TX10p), tropical nights (TR20), percentage of warm nights (TN90p), percentage of cool nights (TN10p), summer days (SU25), cold spell duration indicator (CSDI), hottest days (TXx), warmest nights (TNx), coldest nights (TNn), coldest days (TXn), daily temperature range (DTR). Trend magnitudes are estimated based on Sen's slope estimator.

show an increasing trend with a rate of 0.2°C/ decade and 0.05°C/decade over India from the year 1990. In the case of summer days and tropical nights, they represent a significant positive trend with an increasing rate of ∼0.6 days/decade and 0.9 days/decade (figure 3). Further, the warm nights and warm days also depict an increasing trend at a rate of 2.9°C/decade and 1.5°C/decade. Such intensified night-time temperatures trends can have adverse impacts on crop yield, such as decrease in rice yield based on the study of Peng *et al.* (2004). All warm extremes have exhibited significant increasing trends over the entire western, few parts of central and peninsular India, particularly northwest India (Rajasthan and Gujarat), Maharashtra, Western Ghats, and few parts of Tamil Nadu and Telangana. It is conclusive that all the warm temperature indices show a positive increasing trend over India. The positive changes of temperature extremes obtained in the present study were consistent with the studies of Kumar *et al.* (2020), with about 30% and 32% of India with significant (positive or negative) trends in warm nights per year (TN95) and cold nights per year (TN5), respectively.

5.3 *Dependency between large scale climate indices and precipitation and temperature extreme indices over India*

We have utilized WTC technique to identify the large-scale climate changes in temperature and precipitation extremes and their phase relationships. Table 2 shows the Pearson's correlation coefficients estimated between climate indices and precipitation/temperature indices at annual time scale. The statistically significant ($p < 0.05$) correlation coefficients were estimated between six climate indices and 13 temperature extremes. Among the six climate indices, the ISMI is highly correlated with extreme temperature indices over India. We selected the most significant and highly dependent combination of extreme temperature indices with ISMI for WTC analysis. For example, warm indices such as percentage of warm days, warm spell duration index and hottest days have shown significant negative correlation coefficients as −0.54, −0.56, −0.54, respectively, with ISMI. Whereas, percentage of cool days has shown a significant positive correlation coefficient of 0.46 with ISMI. Therefore, the WTC analysis is
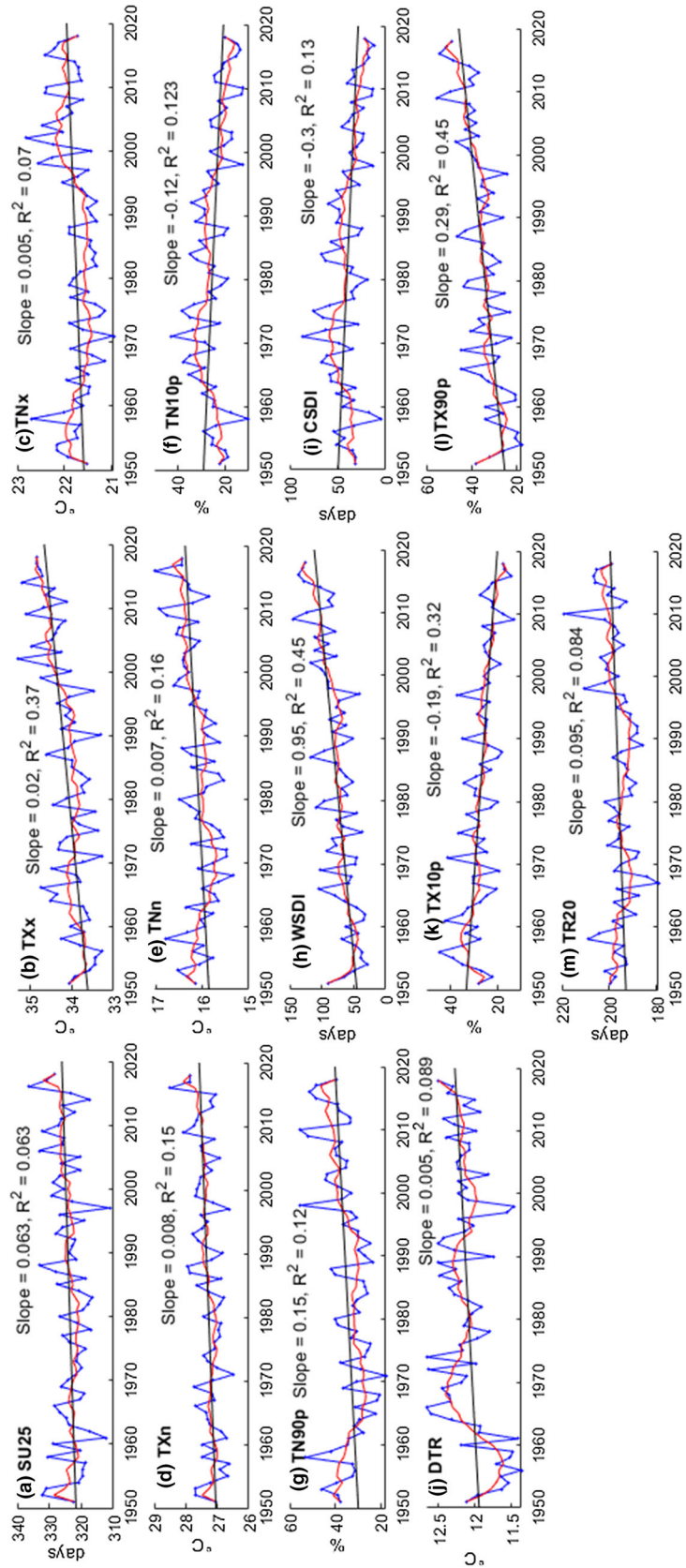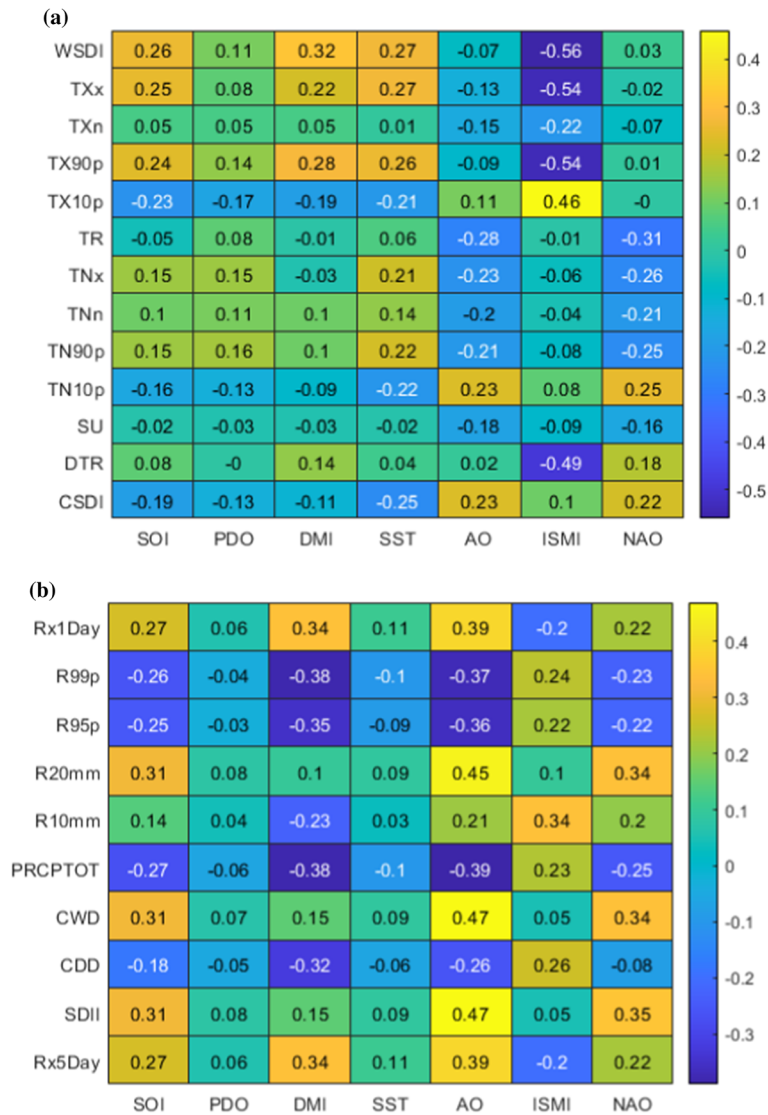
Figure 6. Annual spatial averaged temperature extremes all over India for 1951–2018. The black solid line shows the linear trend line, red colour solid line is 10-yr moving average.

Table 2. *Pearson's correlation coefficients estimated between annual averaged temperature and precipitation extremes and climate indices [Southern Oscillation Index (SOI), Pacific Decadal Oscillation (PDO), Dipole Mode Index (DMI), Arctic Oscillation (AO), North Atlantic Oscillation (NAO), Indian Summer Monsoon Index (ISMI)] all over India for 1951–2018.*

(a)

	SOI	PDO	DMI	SST	AO	ISMI	NAO
WSDI	0.26	0.11	0.32	0.27	-0.07	-0.56	0.03
TXx	0.25	0.08	0.22	0.27	-0.13	-0.54	-0.02
TXn	0.05	0.05	0.05	0.01	-0.15	-0.22	-0.07
TX90p	0.24	0.14	0.28	0.26	-0.09	-0.54	0.01
TX10p	-0.23	-0.17	-0.19	-0.21	0.11	0.46	-0
TR	-0.05	0.08	-0.01	0.06	-0.28	-0.01	-0.31
TNx	0.15	0.15	-0.03	0.21	-0.23	-0.06	-0.26
TNn	0.1	0.11	0.1	0.14	-0.2	-0.04	-0.21
TN90p	0.15	0.16	0.1	0.22	-0.21	-0.08	-0.25
TN10p	-0.16	-0.13	-0.09	-0.22	0.23	0.08	0.25
SU	-0.02	-0.03	-0.03	-0.02	-0.18	-0.09	-0.16
DTR	0.08	-0	0.14	0.04	0.02	-0.49	0.18
CSDI	-0.19	-0.13	-0.11	-0.25	0.23	0.1	0.22

(b)

	SOI	PDO	DMI	SST	AO	ISMI	NAO
Rx1Day	0.27	0.06	0.34	0.11	0.39	-0.2	0.22
R99p	-0.26	-0.04	-0.38	-0.1	-0.37	0.24	-0.23
R95p	-0.25	-0.03	-0.35	-0.09	-0.36	0.22	-0.22
R20mm	0.31	0.08	0.1	0.09	0.45	0.1	0.34
R10mm	0.14	0.04	-0.23	0.03	0.21	0.34	0.2
PRCPTOT	-0.27	-0.06	-0.38	-0.1	-0.39	0.23	-0.25
CWD	0.31	0.07	0.15	0.09	0.47	0.05	0.34
CDD	-0.18	-0.05	-0.32	-0.06	-0.26	0.26	-0.08
SDII	0.31	0.08	0.15	0.09	0.47	0.05	0.35
Rx5Day	0.27	0.06	0.34	0.11	0.39	-0.2	0.22

performed for three warm indices and ISMI combination (TX90p-ISMI, WSDI-ISMI, TXx-ISMI). Figure 7 shows the WTC and phase difference between temperature indices (TX90P, TX10P, WSDI, and TXx) and ISMI. The direction of arrows in the figure represents the phase relationship between the two variables. The arrow pointing up and to the right-in-phase relationship with the tide level leading. The arrow pointing down and to the left-out-of-phase relationship with the tide level leading. ISMI shows a strong signal in 2–3, 2–4 and

6 yrs periodicity with warm days, WSDI, and hottest days, where arrows point left and downwards. The ISMI shows strong signal only in 2–4 yrs periodicity where arrows are pointing right directions. The arrows pointing to the left illustrate the out of phase relationship with ISMI, whereas right arrows indicate the in-phase relation. This seems that variables are negatively correlated or in opposite phase (left arrows). The ISMI lags the temperature indices over Indian region. Overall, ISMI has shown strong influence on temperature
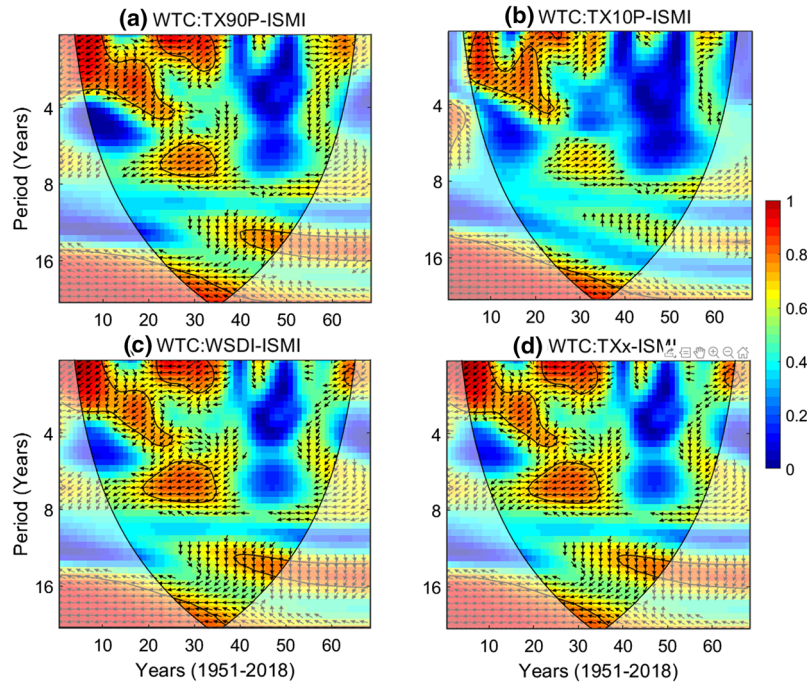
Figure 7. Wavelet coherence and phase difference between temperature extremes and climate indices at an annual time scale over India for the years 1951–2018. Wavelet coherence between percentage of warm days (TX90p) and ISMI (**a**), percentage of cool days (TX10p) and ISMI (**b**), warm spell duration index (WSDI) and ISMI (**c**) and hottest days (TXx) and ISMI (**d**). The thick black contour shows 5% significance level against red noise process.

extremes along with precipitation extremes. The earlier studies have proven that ISMI has a strong influence on precipitation on monthly and annual time scales (e.g., Das *et al.* 2020). It can be noted that the ISMI index is defined based on monsoon season, and the present study compares such monsoon month averaged precipitation index with annual precipitation extreme indices. However, ISMI has shown strong wavelet coherence, representing dominant effect of summer monsoon all over India at annual scales as explained in the study of Das *et al.* (2020). The same study also reveals that wavelet coherence is continuous between ISMI and precipitation at annual scale for the period 1951–2015 all over India, which is in convince with the present study findings.

Similarly, we have also done analysis for precipitation indices with AO (figure 8). The 2–5-yr and 3–5-yr periodicity are dominant in both indices. In both the indices, 2–5 yrs, 3–5-yrs periodicity is dominant. The AO and RX1day and RX5day are in phase relationship, which indicates the AO leads both these indices. Based on earlier studies (Midhuna and Dimri 2019), AO also plays a major role in influencing the winter climate of the Northern Hemisphere as well as the Indian winter monsoon.

From wavelet analysis and wavelet transform coherence analysis, temperature (precipitation)

indices were strongly teleconnected to ISMI (AO) over Indian region. In addition to the influence of large-scale climate patterns, land reclamation, urbanization and other human activities also cause changes in climate extremes (Boyaj *et al.* 2020). These findings will have direct relevance to warming impact over Indian region and suggest an increased probability of enhanced future extremes, impacts, and related risks in a warming climate. The present study is, therefore, an important step towards understanding the joint spatio-temporal signals in the growing collection of droughts due to pronounced changes in extreme precipitation and temperatures, which can be used to understand the near future variability with CMIP6 data sets.

6. Discussion

In recent decades, India has seen an increase in the frequency, duration, and intensity of extreme weather events, resulting in massive loss causalities and economic losses. It is critical to gain knowledge about extremes, which will aid the research community in assessing climate change processes and their impact on various sectors. Based on the current study, extreme precipitation indices spatial variability has been found to be more intense
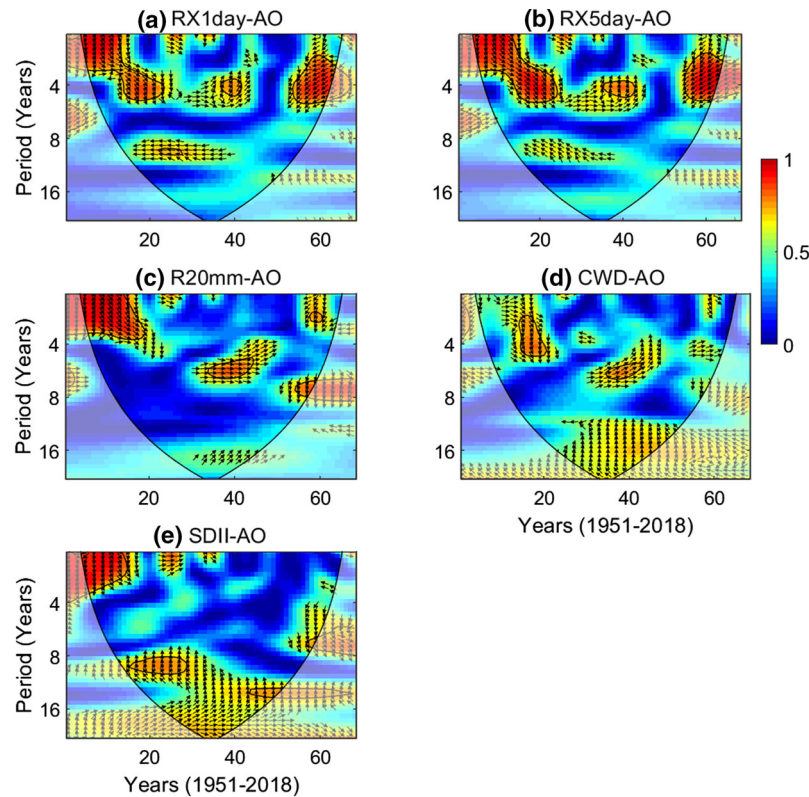
Figure 8. Wavelet coherence and phase difference between precipitation extremes and climate indices at an annual time scale over India for the years 1951–2018. Wavelet coherence between max 1-day precipitation amount (RX1day) and AO (**a**), max 5-day precipitation amount (RX5day) and AO (**b**), number of very heavy precipitation days (R20mm) and AO (**c**), consecutive wet days (CWD) and AO (**d**), simple daily intensity index (SDII) and AO (**e**). The thick black contour shows 5% significance level against red noise process.

towards the Western Ghats and the northeast parts, with more intense dry indices towards the northwestern states of India. The low-pressure systems over the Bay of Bengal and their movement over northern parts of India cause widespread rainfall activity over the central and west coasts of India (Rajeevan and Nayak 2017).

This study reported that most of the precipitation extremes over India had been intensified. The increase in extreme rainfall may be attributed to the increasing variability of the low-level monsoon westerlies in the Arabian Sea (Roxy *et al.* 2017). The increasing trend of extreme precipitation in the Western Ghats is mainly caused by the convective clouds (Maheskumar *et al.* 2014) and offshore troughs and vortices (Francis and Gadgil 2006). Atmospheric rivers and western disturbances are reported to be the causes for wintertime precipitation, whereas tropical lows/tropical depressions are pointed out to be responsible for summer-time extreme precipitation in northern and northeastern India (Yang *et al.* 2018). Increases in extreme precipitation in the tropics are also linked to an increase in mean temperature under

global warming (Rajeevan *et al.* 2008) as well as with urbanization (Kishtawal *et al.* 2010). Furthermore, the increase of precipitation extremes is attributed to increasing trend of sea surface temperature variability and surface latent heat flux over tropical Indian Ocean (Rajeevan *et al.* 2008). Such an increase in precipitation extremes will have an impact on agricultural yield, flash flooding, and ecosystems (Yaduvanshi *et al.* 2021).

This study reported that most of the warm indices have significant increasing trends and decreasing signals of cold indices over India. Such an increase (decrease) in warm (cold) extreme indices was also noted by a few authors at regional scales and all over India independently at coarser resolution (Dash and Mamgain 2011). The present study provides the spatio-temporal trends at finer resolution and coherence of temperature extremes with precipitation indices. It is well known that the change in extreme temperature indices can be attributed to greenhouse gas and aerosol emissions and growing urbanization (Dimri 2019). Decreasing (increasing) trends of cold (warm) days are correlated to the alterations/shifts in rainfall that

cause redistribution of moisture, whereas increments in the frequency of cold days are correlated to the aerosols, especially over Indo-Gangetic plains previously (Ramanathan *et al.* 2007). Intensified changes in extreme temperature indices have an impact on crop yield, production and water resources management (Peng *et al.* 2004). Summer days (SU25), for example, are an environmental factor that can have a negative impact on rainfed crop production (dos Santos *et al.* 2022). It is also evident that, for every increase of 1°C of minimum temperature of about 10% decline in rice grain yield (Peng *et al.* 2004). In this context, global warming and consequent intensification of precipitation and temperature extremes as presented in this study, will have adverse effects on agriculture and water resources with pronounced impacts hydroclimatic extremes such as flash floods, droughts, and heatwaves (Sharma and Mujumdar 2017).

Large-scale climatic indices have a strong influence on hydro-meteorological variables, and it is essential to study the dependence structure for effective climate change predictions. There have been attempts to establish a link between large-scale climatic phenomenon indices and precipitation and temperature extremes both globally and in India (Yadav *et al.* 2013; Xiao *et al.* 2017; Shi and Wang 2019; Das *et al.* 2020). Studies reveal that ISMI is the most effective climatic teleconnection with Indian precipitation at monthly time scales. Furthermore, the present study also showed that ISMI plays a major role on precipitation extremes at annual scales along with warm and cold extreme indices. The AO has also identified a significant teleconnection to impact Indian precipitation extremes (Midhuna and Dimri 2019). El Niño and La Niña events are also found to influence the precipitation and temperature extremes in the previous literature (Alexander *et al.* 2009).

The present study used the most dependable fine-resolution gridded data sets developed based on station-based observations, which is a major limitation of the study. However, the use of *in-situ* station-based observations will provide the most accurate and realistic extremes analysis compared to gridded datasets due to the inherent uncertainties towards the selected interpolation methods and most importantly ability to represent extreme variabilities (King *et al.* 2013; Contractor *et al.* 2015). This provided usability of high-resolution gridded datasets, which are prominent for climate monitoring at national scales; several studies successfully implemented climate extreme analysis based on gridded datasets globally (Alexander and Arblaster 2017) and India (Gupta *et al.* 2020; Kumar *et al.* 2020).

7. Conclusions

The study investigated the analysis of spatio-temporal exploration of precipitation, maximum and minimum temperature extremes over India during 1951–2018, with a view to investigate their association with large scale climate indices. The study looked at the relationship between large-scale climate indices and precipitation and temperature extremes across India. The following major conclusions are derived from this study:

- The spatial climatological average of wet precipitation extreme indices has been found to be more intense towards Western Ghats and northeast parts, while dry precipitation extremes as more intense over northwestern states of India.
- The very wet days (R95) show an increasing trend over India followed by extremely wet days (R99) and simple daily intensity of precipitation (SDII) indices except over Indo-Gangetic region, indicating a climate change signal. Our results showed that the increase in consecutive dry days (CDD) over central India and decrease in consecutive wet days (CWD) throughout India indicate impact of warming over India. Significant increase in the max-5-day precipitation amount (RX5day) over the East Coast of India.
- The decrease in summer days (SU25) over north India may have a significant impact on snow and glacier melting. The increase of hottest days (TXx) shows an increasing trend over India can lead to heat waves, droughts and decline in water resources. Most of the indices show a decreasing pattern, especially over IGP region. The warm extremes have exhibited significant increasing trends over complete western zone, few parts of central and peninsular India, particularly northwest India (Rajasthan and Gujarat), Maharashtra, Western Ghats, and few parts of Tamil Nadu and Telangana.
- The cold indices, such as coldest days and nights have increased over the past 68 years, specifically over northwest (Rajasthan and Gujarat), Maharashtra, Western Ghats, and few parts of Tamil Nadu. Whereas, extremes such as cool nights, cold spells, and cool days have shown decreasing signals all over India.

- The extreme warm indices (percentage of warm days, warm spell duration index, and hottest days) were negatively connected with ISMI and positively connected with extreme cold index (percentage of cool days).

- Our results suggest that warming and moistening of the atmosphere may affect the spatial extent of the precipitation over the Indian region.

- The relationship between teleconnections of temperature/precipitation variability and extremes is significantly strong over India. Temperature (precipitation) indices were strongly teleconnected to ISMI (AO). The strong influence of teleconnections on the characteristics of precipitation extremes also suggests a potentially higher magnitude of changes as a response to rising temperature.

- The high dependence of precipitation and temperature extremes with large-scale climate indices indicates high vulnerability to extremes under climate change.

Acknowledgements

Author statement

S Rehana: Conceptualization, methodology, original draft preparation. Pranathi Yeleswarapu: Data curation, software, visualization. Ghouse Basha: Methodology, investigation, reviewing and editing. Francisco Munoz-Arriola: Supervision, investigation, reviewing and editing.

References

Alexander L V 2016 Global observed long-term changes in temperature and precipitation extremes: A review of progress and limitations in IPCC assessments and beyond; *Weather Clim. Extrem.* **11** 4–16, https://doi.org/10.1016/j.wace.2015.10.007.

Alexander L V and Arblaster J M 2017 Historical and projected trends in temperature and precipitation extremes in Australia in observations and CMIP5; *Weather Clim. Extrem.* **15** 34–56, https://doi.org/10.1016/j.wace.2017.02.001.

Alexander L V, Uotila P and Nicholls N 2009 Influence of sea surface temperature variability on global temperature and precipitation extremes; *J. Geophys. Res. Atmos.* **114**, https://doi.org/10.1029/2009JD012301.

Boyaj A, Dasari H P, Hoteit I and Ashok K 2020 Increasing heavy rainfall events in south India due to changing land use and land cover; *Quart. J. Roy. Meteorol. Soc.* **146** 3064–3085, https://doi.org/10.1002/qj.3826.

Chandrashekar V D and Shetty A 2018 Trends in extreme rainfall over ecologically sensitive Western Ghats and coastal regions of Karnataka: An observational assessment; *Arab. J. Geosci.* **11** 327, https://doi.org/10.1007/s12517-018-3700-6.

Contractor S, Alexander L V, Donat M G and Herold N 2015 How Well Do Gridded Datasets of Observed Daily Precipitation Compare over Australia?; *Adv. Meteorol.* **2015** e325718, https://doi.org/10.1155/2015/325718.

Curry C L, Sillmann J, Bronaugh D, Alterskjaer K, Cole J N S, Ji D, Kravitz B, Kristjánsson J E, Moore J C, Muri H, Niemeier U, Robock A, Tilmes S and Yang S 2014 A multimodel examination of climate extremes in an idealized geoengineering experiment; *J. Geophys. Res. Atmos.* **119** 3900–3923, https://doi.org/10.1002/2013JD020648.

Das J and Nanduri U V 2018 Future Projection of precipitation and temperature extremes using change factor method over a river basin: Case study; *J. Hazard Toxic Radioact. Waste* **22** 04018006, https://doi.org/10.1061/(ASCE)HZ.2153-5515.0000399.

Das J, Jha S and Goyal M K 2020 On the relationship of climatic and monsoon teleconnections with monthly precipitation over meteorologically homogenous regions in India: Wavelet and global coherence approaches; *Atmos. Res.* **238** 104889, https://doi.org/10.1016/j.atmosres.2020.104889.

Dash S K and Mamgain A 2011 Changes in the frequency of different categories of temperature extremes in India; *J. Appl. Meteorol. Climatol.* **50** 1842–1858, https://doi.org/10.1175/2011JAMC2687.1.

Deshpande N R, Kothawale D R and Kulkarni A 2016 Changes in climate extremes over major river basins of India; *Int. J. Climatol.* **36** 4548–4559, https://doi.org/10.1002/joc.4651.

Dimri A P 2019 Comparison of regional and seasonal changes and trends in daily surface temperature extremes over India and its subregions; *Theor. Appl. Climatol.* **136** 265–286, https://doi.org/10.1007/s00704-018-2486-5.

Donat M G, Alexander L V, Yang H, Durre I, Vose R, Dunn R J H, Willett K M, Aguilar E, Brunet M, Caesar J, Hewitson B, Jack C, Klein Tank A M G, Kruger A C, Marengo J, Peterson T C, Renom M C, Rojas Oria, Rusticucci M, Salinger J, Elrayah A S, Sekele S S, Srivastava A K, Trewin B, Villarroel C, Vincent L A, Zhai P, Zhang X and Kitching S 2013 Updated analyses of temperature and precipitation extreme indices since the beginning of the twentieth century; The HadEX2 dataset; *J. Geophys. Res. Atmos.* **118** 2098–2118, https://doi.org/10.1002/jgrd.50150.

dos Santos C A C, Neale C M U, Mekonnen M M, Gonçalves I Z, de Oliveira G, Ruiz-Alvarez O, Safa B and Rowe C M 2022 Trends of extreme air temperature and precipitation

and their impact on corn and soybean yields in Nebraska, USA; *Theor. Appl. Climatol.*, https://doi.org/10.1007/s00704-021-03903-7.

Francis P A and Gadgil S 2006 Intense rainfall events over the west coast of India; *Meteorol. Atmos. Phys.* **94** 27–42, https://doi.org/10.1007/s00703-005-0167-2.

Ghosh S, Das D, Kao S-C and Ganguly A R 2012 Lack of uniform trends but increasing spatial variability in observed Indian rainfall extremes; *Nat. Clim. Change* **2** 86–91, https://doi.org/10.1038/nclimate1327.

Gilbert R O 1987 *Statistical methods for environmental pollution monitoring*; John Wiley & Sons, Van Nostrand Reinhold Company Limited, New York, ISBN: 978-0-471-28878-7.

Gupta V, Singh V and Jain M K 2020 Assessment of precipitation extremes in India during the 21st century under SSP1-1.9 mitigation scenarios of CMIP6 GCMs; *J. Hydrol.* **590** 125422, https://doi.org/10.1016/j.jhydrol.2020.125422.

Hirsch R M, Slack J R and Smith R A 1982 Techniques of trend analysis for monthly water quality data; *Water Resour. Res.* **18** 107–121, https://doi.org/10.1029/WR018i001p00107.

Irannezhad M, Liu J and Chen D 2020 Influential climate teleconnections for spatio-temporal precipitation variability in the Lancang-Mekong river basin from 1952 to 2015; *J. Geophys. Res. Atmos.* **125** e2020JD033331, https://doi.org/10.1029/2020JD033331.

Jena P, Kasiviswanathan K S and Azad S 2020 Spatio-temporal characteristics of extreme droughts and their association with sea surface temperature over the Cauvery River basin, India; *Nat. Hazards* **104** 2239–2259, https://doi.org/10.1007/s11069-020-04270-8.

Kendall M G 1955 *Rank correlation methods*; Charles Griffin & Co. Ltd., London.

Khan M, Munoz-Arriola F, Rehana S and Greer P 2019 Spatial heterogeneity of temporal shifts in extreme precipitation across India; *J. Clim. Change* **5** 19–31, https://doi.org/10.3233/JCC190003.

King A D, Alexander L V and Donat M G 2013 The efficacy of using gridded data to examine extreme rainfall characteristics: a case study for Australia; *Int. J. Climatol.* **33** 2376–2387, https://doi.org/10.1002/joc.3588.

Kishtawal C, Niyogi D, Tewari M,Pielke Sr R A and Shepherd J M 2010 Urbanization signature in the observed heavy rainfall climatology over India; *Int. J. Climatol.* **30**, https://doi.org/10.1002/joc.2044.

Kumar S, Chanda K and Pasupuleti S 2020 Spatio-temporal analysis of extreme indices derived from daily precipitation and temperature for climate change detection over India; *Theor. Appl. Climatol.* **140** 343–357, https://doi.org/10.1007/s00704-020-03088-5.

Lin P, He Z, Du J, Chen L, Shu X and Li J 2017 Recent changes in daily climate extremes in an arid mountain region, a case study in northwestern China's Qilian Mountains; *Sci. Rep.* **7** 2245, https://doi.org/10.1038/s41598-017-02345-4.

Maheskumar R S, Narkhedkar S G, Morwal S B, Padmakumari B, Kothawale D R, Joshi R R, Deshpande C G, Bhalwankar R V and Kulkarni J R 2014 Mechanism of high rainfall over the Indian west coast region during the monsoon season; *Clim. Dyn.* **43** 1513–1529, https://doi.org/10.1007/s00382-013-1972-9.

Mann H B 1945 Nonparametric tests against trend; *Econometrica* **13** 245, https://doi.org/10.2307/1907187.

Midhuna T M and Dimri A P 2019 Impact of arctic oscillation on Indian winter monsoon; *Meteorol. Atmos. Phys.* **131** 1157–1167, https://doi.org/10.1007/s00703-018-0628-z.

Mishra V, Ganguly A R, Nijssen B and Lettenmaier D P 2015 Changes in observed climate extremes in global urban areas; *Environ. Res. Lett.* **10** 024005, https://doi.org/10.1088/1748-9326/10/2/024005.

Murari K K, Gosh S, Patwardhan A, Daly E and Salvi K 2015 Intensification of future severe heat waves in India and their effect on heat stress and mortality; *Region. Environ. Change* **15** 569–579, https://doi.org/10.1007/s10113-014-0660-6.

Pai D S, Rajeevan M, Sreejith O P, Mukhopadhyay B and Satbha N S 2014 Development of a new high spatial resolution (0.25° × 0.25°) long period (1901–2010) daily gridded rainfall data set over India and its comparison with existing data sets over the region; *Mausam* **65(1)**, https://doi.org/10.54302/mausam.v65i1.851.

Panda D K, Panigrahi P, Mohanty S and Sethi R R 2016 The 20th century transitions in basic and extreme monsoon rainfall indices in India: Comparison of the ETCCDI indices; *Atmos. Res.* **181** 220–235, https://doi.org/10.1016/j.atmosres.2016.07.002.

Panda D K, Aghakouchak A and Ambast S 2017 Increasing heat waves and warm spells in India, observed from a multi-aspect framework; *J. Geophys. Res. Atmos.* **122** 7, https://doi.org/10.1002/2016JD026292.

Peng S, Huang J, Sheehy J E, Laza R C, Visperas R M, Zhong X, Centeno G S, Khush G S and Cassman K G 2004 Rice yields decline with higher night temperature from global warming; *Proc. Natl. Acad Sci.* **101** 9971–9975, https://doi.org/10.1073/pnas.0403720101.

Rai P, Choudhary A and Dimri A P 2019 Future precipitation extremes over India from the CORDEX-South Asia experiments; *Theor. Appl. Climatol.* **137** 2961–2975, https://doi.org/10.1007/s00704-019-02784-1.

Rajeevan M N and Nayak S 2017 *Observed climate variability and change over the Indian region*; Springapore, https://doi.org/10.1007/978-981-10-2531-0.

Rajeevan M, Bhate J and Jaswal A K 2008 Analysis of variability and trends of extreme rainfall events over India using 104 years of gridded daily rainfall data; *Geophys. Res. Lett.* **35**, https://doi.org/10.1029/2008GL035143.

Ramanathan V, Ramana M V, Roberts G, Kim D, Corrigan C, Chung C and Winker D 2007 Warming trends in Asia amplified by brown cloud solar absorption; *Nature* **448** 575–578, https://doi.org/10.1038/nature06019.

Ratnam J V, Behera S K, Ratna S B, Rajeevan M and Yamagata T 2016 Anatomy of Indian heatwaves; *Sci. Rep.* **6** 24395, https://doi.org/10.1038/srep24395.

Rehana S and Monish N T 2020 Characterization of regional drought over water and energy limited zones of India using potential and actual evapotranspiration; *Earth Space Sci.* **7** e2020EA001264, https://doi.org/10.1029/2020EA001264.

Rehana S and Monish N T 2021 Impact of potential and actual evapotranspiration on drought phenomena over water and energy-limited regions; *Theor. Appl. Climatol.* **144** 215–238, https://doi.org/10.1007/s00704-021-03521-3.

Rohini P, Rajeevan M and Srivastava A K 2016 On the variability and increasing trends of heat waves over India; *Sci. Rep.* **6** 26153, https://doi.org/10.1038/srep26153.

Roxy M K, Ghosh S, Pathak A, Athulya R, Mujumdar M, Murtugudde R, Terray P and Rajeevan M 2017 A threefold rise in widespread extreme rain events over central India; *Nat. Commun.* **8** 708, https://doi.org/10.1038/s41467-017-00744-9.

Roy S S 2019 Spatial patterns of trends in seasonal extreme temperatures in India during 1980–2010; *Weather Clim. Extrem.* **24** 100203, https://doi.org/10.1016/j.wace.2019.100203.

Sen P K 1968 Estimates of the regression coefficient based on Kendall's Tau; *J. Am. Stat. Assoc.* **63** 1379–1389, https://doi.org/10.1080/01621459.1968.10480934.

Sharma S and Mujumdar P 2017 Increasing frequency and spatial extent of concurrent meteorological droughts and heatwaves in India; *Sci. Rep.* **7** 1–9, https://doi.org/10.1038/s41598-017-15896-3.

Shi H and Wang B 2019 How does the Asian summer precipitation-ENSO relationship change over the past 544 years? *Clim. Dyn.* **52** 4583–4598, https://doi.org/10.1007/s00382-018-4392-z.

Torrence C and Compo G P 1998 A practical guide to wavelet analysis; *Bull. Am. Meteorol. Soc.* **79** 61–78, https://doi.org/10.1175/1520-0477(1998)079%3c0061:APGTWA%3e2.0.CO;2.

Utsumi N, Seto S, Kanae S, Maeda E E and Oki T 2011 Does higher surface temperature intensify extreme precipitation?; *Geophys. Res. Lett.* **38**, https://doi.org/10.1029/2011GL048426.

Vinnarasi R and Dhanya C T 2016 Changing characteristics of extreme wet and dry spells of Indian monsoon rainfall; *J.*

Geophys. Res. Atmos.* **121** 2146–2160, https://doi.org/10.1002/2015JD024310.

Vinnarasi R, Dhanya C T, Chakravorty A and AghaKouchak A 2017 Unravelling diurnal asymmetry of surface temperature in different climate zones; *Sci. Rep.* **7** 7350, https://doi.org/10.1038/s41598-017-07627-5.

Xiao M, Zhang Q and Singh V P 2017 Spatiotemporal variations of extreme precipitation regimes during 1961–2010 and possible teleconnections with climate indices across China; *Int. J. Climatol.* **37** 468–479, https://doi.org/10.1002/joc.4719.

Yadav R K, Ramu D A and Dimri A P 2013 On the relationship between ENSO patterns and winter precipitation over North and Central India; *Glob. Planet. Change* **107** 50–58, https://doi.org/10.1016/j.gloplacha.2013.04.006.

Yaduvanshi A, Nkemelang T, Bendapudi R and New M 2021 Temperature and rainfall extremes change under current and future global warming levels across Indian climate zones; *Weather Clim. Extrem.* **31** 100291, https://doi.org/10.1016/j.wace.2020.100291.

Yang Y, Zhao T, Ni G and Sun T 2018 Atmospheric rivers over the Bay of Bengal lead to northern Indian extreme rainfall; *Int. J. Climatol.* **38** 1010–1021, https://doi.org/10.1002/joc.5229.

Zhang X, Alexander L, Hegerl G C, Jones P, Tank A K, Peterson T C, Trewin B and Zwiers F W 2011 Indices for monitoring changes in extremes based on daily temperature and precipitation data; *Wires Clim. Change* **2** 851–870, https://doi.org/10.1002/wcc.147.